

# Hydrogen sensing properties of dielectrophoretically assembled SnO<sub>2</sub> nanoparticles on CMOS-compatible micro-hotplates

Youngreal Kwak<sup>1</sup>, Jianwei Wang<sup>1</sup>, Sunglyul Meang<sup>2</sup> and Gil-Ho Kim<sup>1</sup>

<sup>1</sup> Department of Electronic and Electrical Engineering, and Sungkyunkwan University Advanced Institute of Nanotechnology, Sungkyunkwan University, Suwon 440-746, Republic of Korea

<sup>2</sup> Department of Electronic and Electrical Engineering, Woosuk University, Wanju, Jeollabuk-do 565-701, Republic of Korea

E-mail: [ghkim@skku.edu](mailto:ghkim@skku.edu)

Received 4 May 2011, in final form 14 June 2011

Published 11 October 2011

Online at [stacks.iop.org/Nano/22/445501](http://stacks.iop.org/Nano/22/445501)

## Abstract

We fabricated nanoparticle-based gas through *in situ* ac dielectrophoretic assembling of drop-coated SnO<sub>2</sub> nanoparticles to bridge the gap between electrodes with high aspect ratio. While the conventional dielectrophoresis (DEP) adopts a microfluidic system for continuous flow of the solution during the process, we just drop-coated a small amount of solution onto the electrodes and executed *in situ* DEP for a very short time. This is a very simple, cost-effective, time-saving, and highly reproducible process. We fixed the duration time and applied voltage for the DEP at 1 s and 1 V respectively and changed the frequencies from 1 up to 500 kHz. *I*–*V* characteristics of the samples were checked and it was found that DEP samples fabricated at 1 s, 1 V and 150 kHz conditions showed considerably higher connectivity of the nanoparticles. This can be attributed to the excellent step coverage achieved by ac DEP under those conditions. The devices drop-coated and dielectrophoretically assembled at other ac frequency conditions showed poor connectivity. Hydrogen gas sensing properties of the sensors fabricated under 1 s, 1 V and 150 kHz conditions were checked by flowing through 160 ppm H<sub>2</sub>. The sensitivity reaches a maximum value of ~700% at 350 °C. The response time is ~200 s at 350 °C.

(Some figures in this article are in colour only in the electronic version)

## 1. Introduction

Today, hydrogen is becoming an increasingly important resource as an environment-friendly fuel. Due to its potential hazard by leakage, the development of highly sensitive hydrogen detecting systems has been requested [1, 2]. For hydrogen gas sensing applications, tin dioxide (SnO<sub>2</sub>) has long been considered and extensively studied [3–6]. Polycrystalline SnO<sub>2</sub> gas sensors based on porous pellets or thick films were first commercialized [7–9]. Due to low surface-to-bulk ratio, the polycrystalline sensing materials exhibit poor sensitivity. Furthermore, they are not suitable for the integration in

the fabrication of intelligent microsensors. Nanocrystalline SnO<sub>2</sub> thin films fabricated by physical vapor deposition (PVD) or chemical vapor deposition (CVD) were developed later [10–15]. Even though these materials show very high sensitivity and microsensor compatibility, the deposition process requires a high vacuum system and, thus, is not so cost-effective. Recently, SnO<sub>2</sub> nano-powders obtained by the sol–gel process have been proposed as very cheap and highly sensitive sensing materials [16–22]. These materials are normally dip- or spin-coated on planar-type interdigitated electrodes (IEDs) of the sensor platform. The sensor response of hydrogen is known to decrease monotonically with

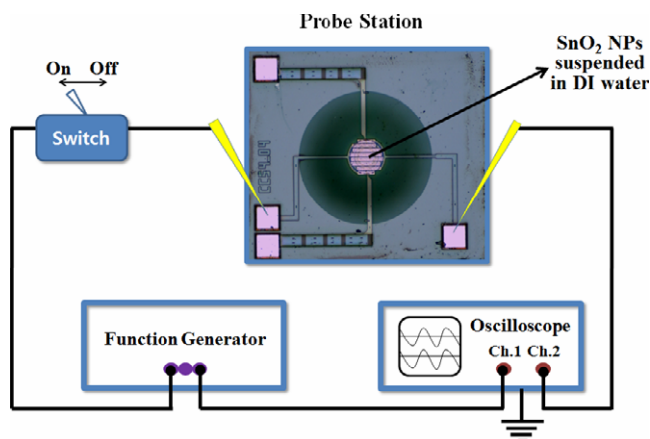


**Figure 1.** Schematic diagram of the setup used for the ac DEP assembly of SnO<sub>2</sub> nanoparticles on IEDs.

increasing the nanocrystalline SnO<sub>2</sub> film thickness [19]. Thus, development of ultra-thin film deposition of nanocrystalline SnO<sub>2</sub> is requested for high grade hydrogen gas sensor applications.

As a method of ultra-thin deposition of nanomaterials, ac dielectrophoresis (DEP) has been proposed and applied to fabricate nanomaterial-based gas sensors [23–28]. Even though the ac DEP technique secures relatively good reproducibility, it is very complicated and costly due to requirements of microchannels, syringe pumps, and specially designed electrodes. A rather simple and cheap ac dielectrophoresis was proposed for thick film SnO<sub>2</sub> gas sensor fabrication by Gardeshzadeh *et al* [29]. However, ultra-thin film SnO<sub>2</sub> nanoparticle deposition by using ac DEP has never been attempted.

In this paper, we report for the first time a new simple technique of ultra-thin sensing material *in situ* deposition which shows advantages of both drop-coating and conventional ac DEP techniques. By using this technique, we fabricated CMOS-compatible microsensors for hydrogen gas detection which showed very high sensitivity and reproducibility.

## 2. Experimental details

Tin oxide nano-powders were obtained by a wet chemical method from a SnCl<sub>4</sub> solution. The precursor chloride (3.5 g SnCl<sub>4</sub>·5H<sub>2</sub>O) dissolved in methanol (100 ml) was precipitated, by adding an ammonia solution (4 ml NH<sub>4</sub>OH), to hydrate SnO<sub>2</sub>. Filtering and washing of the resulting solution to remove large clusters and impurities were followed by drying process over 80 °C for 5 h. The tin oxide powders were then calcined in air at 400 °C for 2 h. The grain size of the powder was observed by scanning electron microscopy (SEM) (JEOL, Model: JSM-7401F).

The calcined tin oxide nano-powders were dispersed in de-ionized (DI) water with the volume ratio of 1:100. The SnO<sub>2</sub> nanoparticles formed agglomerates in the solution. Hence, ultrasonication of the solution was carried out for 10 min to separate the agglomerates into individual nanoparticles. After packaging and wire bonding of micro-hotplates, the

**Table 1.** The conditions of applied current and voltage for respective temperatures.

Temperature (°C)	Voltage (V)	Current (mA)	Power (mW)
100	0.5	7.0	3.5
150	0.7	9.0	6.3
200	1.0	10.0	10.0
250	1.2	11.5	13.8
300	1.3	12.5	16.3
350	1.5	13.5	20.25
400	1.7	14.0	23.8
450	1.8	14.5	26.1
500	2.0	15.0	30.0

*in situ* ac dielectrophoresis was performed on the interdigitated electrodes (IEDs) of the micro-hotplates, details of which have been described elsewhere [30].

0.1 μl of the SnO<sub>2</sub> nanoparticles solution was first drop-coated onto the IEDs of the micro-hotplates by micropipette. Then *in situ* ac DEPs were carried out by using a function generator (Tektronix, Model: AFG3102-R5) at 1 V for 1 s by varying ac frequencies from 1 to 500 kHz. Figure 1 shows the schematic diagram of *in situ* ac DEP. After the DEP process, the devices were dried up by heating the micro-hotplates over 400 °C for 10 min. The patterns of ultra-thin SnO<sub>2</sub> nanoparticle layers deposited onto IED were investigated by optical microscopy (Olympus, Model: BX41M-LED) and atomic force microscopy (AFM) (SII, Model: SPA-300HV). The current–voltage (*I*–*V*) characteristics of the devices were checked by using a *I*–*V* measurement system (Keithley, Model: SCS-4200).

Devices were placed in a gas reaction chamber and connected with the *I*–*V* measurement system. To supply the power to the micro-hotplates a circuit which consists of a battery and a variable resistor was designed. The gas sensing was done in a vacuum chamber by flowing 20 sccm hydrogen gas. The concentration of the gas is fixed to 160 ppm. The resistance of the devices was checked by using a *I*–*V* measurement system from 100 up to 500 °C at intervals of 50°. Table 1 shows the conditions of applied current and voltage for respective temperatures.

## 3. Results and discussions

Figure 2 shows the SEM image of calcined tin oxide nano-powders. As shown in figure 2 the synthesized nanoparticle size is between 20 nm and 40 nm (average ~30 nm). This size is bigger than that estimated by Diéguez *et al* [17]. Figure 3 shows optical images of the assembled SnO<sub>2</sub> nanoparticles on IEDs of micro-hotplates with 4 μm gap electrodes when the DEP was carried out at various frequencies: (a) 1, (b) 100, (c) 150 and (d) 500 kHz keeping applied peak-to-peak voltage and time at 1 V and 1 s, respectively. Figure 4 exhibits the *I*–*V* characteristics of the devices fabricated at different ac DEP frequency conditions. The very low current level (~10<sup>-10</sup> A) at 1 kHz indicates that the DEP was inactive; the dielectrophoretic assembling of nanoparticles did not take place. The current levels were observed to increase at other ac

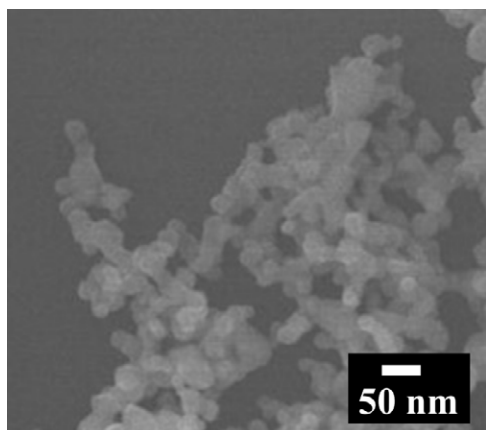


Figure 2. SEM images of calcined tin oxide nanoparticles.

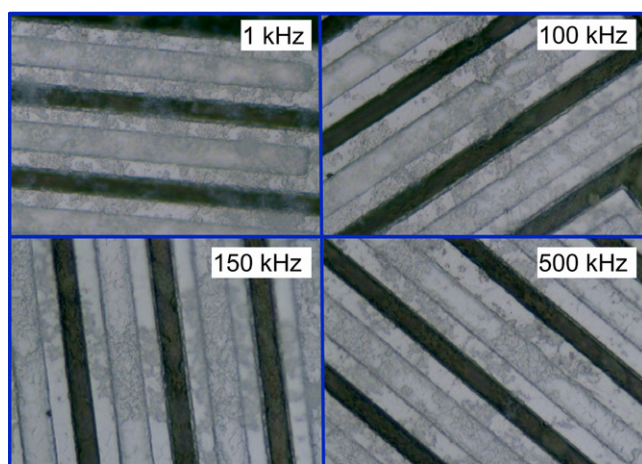


Figure 3. Optical images of dielectrophoretically assembled  $\text{SnO}_2$  nanoparticles on IEDs of micro-hotplates at (a) 1, (b) 100, (c) 150 and (d) 500 kHz ac DEP frequency conditions.

DEP frequency conditions and maximized at 150 kHz. This implies that DEP is most active at 150 kHz.

Figure 5 shows an AFM image of the IEDs dielectrophoretically assembled with  $\text{SnO}_2$  nanoparticles at 150 kHz. This AFM image shows that the IEDs have a very high aspect ratio which hinders the good step coverage of drop-coated nanoparticles. By *in situ* ac DEP at 150 kHz, the  $\text{SnO}_2$  nanoparticles seem to efficiently spread all over the IED patterns with excellent connectivity. The high aspect ratio is due to the 1  $\mu\text{m}$ -thick  $\text{SiN}_x$  passivation layer which covers both the CMOS and IEDs. As long as the sensor platform technology pursues the CMOS-compatibility, this high aspect ratio is inevitable. Many authors who had fabricated nanomaterial-based gas sensors by the drop-coating method reported good results [31–33]. Normally the authors introduced IED structure of very low aspect ratio with which the step coverage problem is not so important. The introduction of very low aspect ratio IEDs, however, cannot be facilitated in fabricating standard CMOS-compatible microsensors.

Figure 6 shows the normalized sensing response of the device fabricated at 150 kHz ac DEP when exposed to 160 ppm  $\text{H}_2$  gas. Here the normalized sensing response is defined as

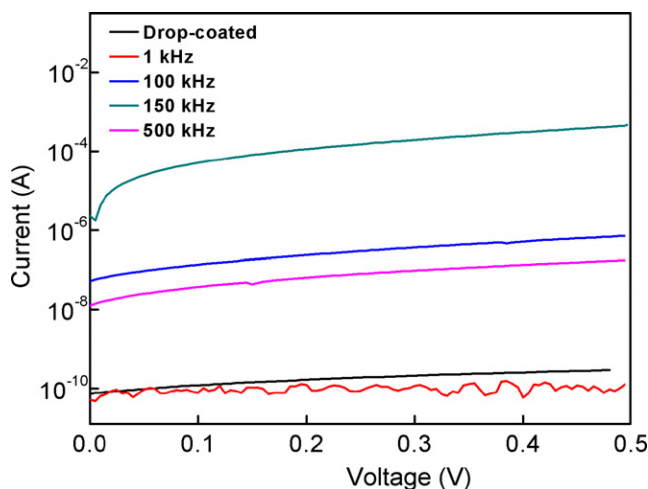


Figure 4.  $I$ - $V$  characteristics of the devices fabricated at different ac DEP frequency conditions.

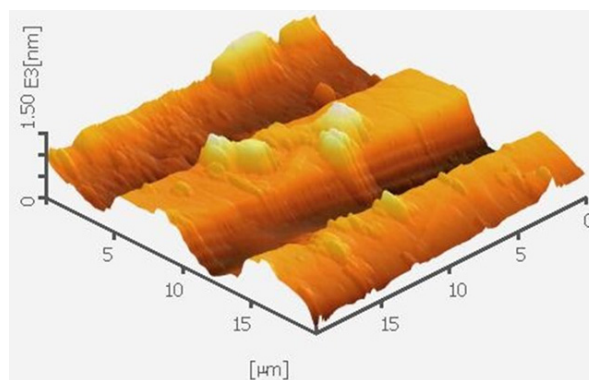


Figure 5. AFM image of the IEDs dielectrophoretically assembled with  $\text{SnO}_2$  nanoparticles at 150 kHz.

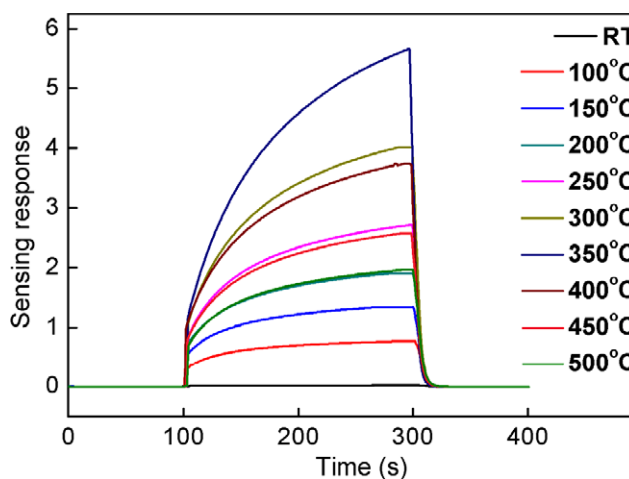
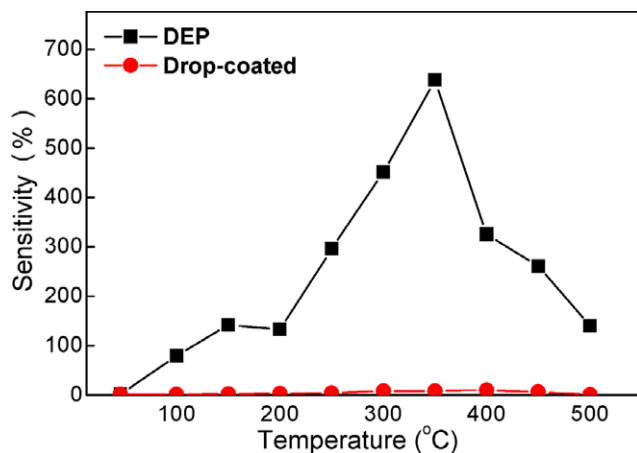
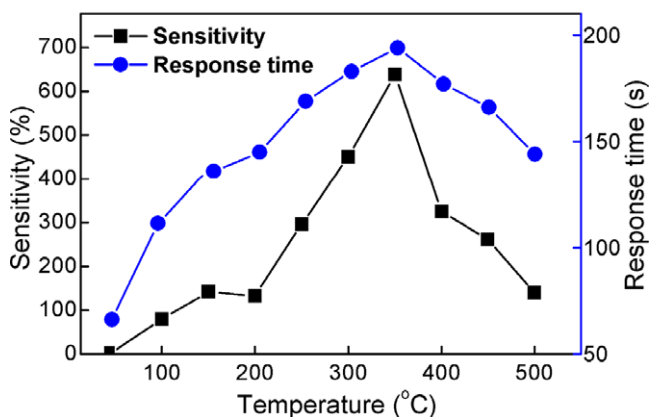


Figure 6. Normalized sensing response ( $(R_0 - R_{\text{H}_2})/R_{\text{H}_2}$  where  $R_0$  indicates the baseline resistance and  $R_{\text{H}_2}$  the resistance of the device exposed to  $\text{H}_2$  gas) of a device exposed to 160 ppm  $\text{H}_2$  gas at various temperatures.

$(R_0 - R_{\text{H}_2})/R_{\text{H}_2}$  where  $R_0$  indicates the baseline resistance and  $R_{\text{H}_2}$  the resistance of the device exposed to  $\text{H}_2$  gas. Figure 7 shows the hydrogen sensitivity of the device measured at



**Figure 7.** The hydrogen sensitivity of a device fabricated by using ac DEP is compared with that of a device fabricated by the drop-coating process at various temperature ranges.



**Figure 8.** Response time (until resistance drops by 90% when H<sub>2</sub> gas is introduced into the gas reaction chamber) and sensitivity versus temperature.

various temperature ranges. Here the sensitivity is defined as the attainable maximum sensing response (%) at a certain H<sub>2</sub> concentration. As shown in this figure the sensitivity of the device fabricated at the 150 kHz ac DEP condition reaches up to 600–700% at 350 °C for 160 ppm H<sub>2</sub>. These values can be compared to those obtained by other researchers to conclude that the *in situ* DEP method achieves a highly sensitive H<sub>2</sub> sensor [11, 15, 18–20, 34]. The very poor sensitivity of the device fabricated by the drop-coating process is due to the very low connectivity of SnO<sub>2</sub> nanoparticles.

Figure 8 shows the sensor response time coupled with the sensitivity for various temperatures. Here the sensor response time is defined as the time for the resistance to drop by 90% of the initial baseline resistance when H<sub>2</sub> gas is introduced. As shown in this figure, the sensor response time of the device is 50–200 s and tends to decrease when the sensitivity increases. The response time of a conventional thin film SnO<sub>2</sub> gas sensor is reported to be more than 1000 s for the same amount of H<sub>2</sub> gas [15, 35].

In figure 9, the sensitivities of three different devices which were fabricated at 150 kHz ac DEP conditions are compared to see the reproducibility of the proposed

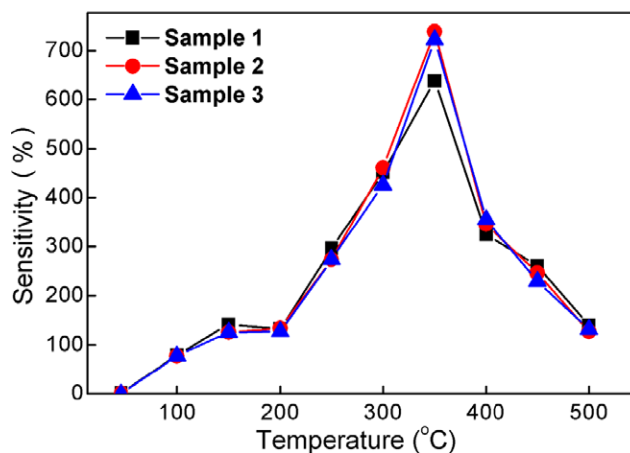


**Figure 9.** Sensitivities of three different devices which were fabricated by ac DEP under the same conditions.

manufacturing process. The sensitivity of each device almost coincides with small variations for all temperature ranges experimentally checked out. This indicates that the *in situ* ac DEP process is highly reproducible.

#### 4. Conclusion

We fabricated a novel gas sensor, in which web-like ultra-thin bridges of SnO<sub>2</sub> nanoparticles were assembled between electrodes having high aspect ratio through *in situ* ac DEP. While the gas sensor fabricated by the drop-coating method did not work properly, that fabricated by *in situ* ac DEP showed very high sensitivity. This can be attributed to the excellent step coverage achieved by ac DEP. The fabrication processes do not involve complicated, expensive or time consuming steps. The sensitivity for 160 ppm H<sub>2</sub> reaches a maximum value of ~700% at 350 °C. Our sensor has similar or even higher sensitivity to H<sub>2</sub> gas compared with different types of SnO<sub>2</sub>-based gas sensors. The sensor response time of the device is 50–200 s, which is much shorter than conventional thin film SnO<sub>2</sub> gas sensors. By comparing three sensors fabricated under the same ac DEP conditions, we showed that the fabrication method is highly reproducible.

#### Acknowledgments

This research was supported by the WCU (World Class University) program through the National Research Foundation of Korea (NRF) funded by the Ministry of Education, Science and Technology (Grant No. R32-2008-000-10204-0). This research was also supported by Woosuk University and the RIC program of MKE in Woosuk University.

#### References

- [1] Christofides C and Mandelis A 1990 *J. Appl. Phys.* **68** R1
- [2] Shukla S, Seal S, Ludwig L and Parish C 2004 *Sensors Actuators B* **97** 256
- [3] Katsuki A and Fukui K 1998 *Sensors Actuators B* **52** 30
- [4] Sheng L Y, Tang Z, Wu J, Chan C H P and Sin K O J 1998 *Sensors Actuators B* **49** 81

- [5] Chaudhary V A, Mulla I S and Vijayamohan K 1999 *Sensors Actuators B* **55** 154
- [6] Niranjana R S, Hwang Y K, Kim D K, Jung S H, Chang J S and Mulla I S 2005 *Mater. Chem. Phys.* **92** 384
- [7] Labeau M, Schmatz U, Delabouglise G, Roman J, Vallet M R and Gaskov A 1995 *Sensors Actuators B* **26** 49
- [8] Martinelli G and Carotta M C 1995 *Sensors Actuators B* **23** 157
- [9] Ansari S G, Gosavi S W, Gangal S A, Karekar R N and Aiyer R C 1997 *J. Mater. Electron.* **8** 23
- [10] Sberveglieri G 1992 *Sensors Actuators B* **6** 239
- [11] Ansari S G, Boroojerdian P, Sainkar S R, Karekar R N, Aiyer R C and Kulkarni S K 1997 *Thin Solid Films* **295** 271
- [12] Carbajal F G, Tiburcio S A, Domínguez J M and Sánchez J A 2000 *Thin Solid Films* **373** 141
- [13] Brown J R, Haycock P W, Smith L M, Jones A C and Williams E W 2000 *Sensors Actuators B* **63** 109
- [14] Ivanov P, Llobet E, Vergara A, Stankova M, Vilanova X, Hubalek J, Gracia I, Cané C and Correig X 2005 *Sensors Actuators B* **111/112** 63
- [15] Lassesson A, Schulze M, Lith J V and Brown A 2008 *Nanotechnology* **19** 015502
- [16] Rella R, Serra A, Siciliano P, Vasanelli L, De G, Licciulli A and Quirini A 1997 *Sensors Actuators B* **44** 462
- [17] Diéguez A, Romano-Rodríguez A, Morante J R, Kappler J, Bârsan N and Göpel W A 1999 *Sensors Actuators B* **60** 125
- [18] Lu F, Liu Y, Dong M and Wang X 2000 *Sensors Actuators B* **66** 225
- [19] Sakai G, Baik N S, Miura N and Yamazoe N 2001 *Sensors Actuators B* **77** 116
- [20] Shukla S, Patil S, Kuiry S C, Rahman Z, Du T, Ludwig L, Parish C and Seal S 2003 *Sensors Actuators B* **96** 343
- [21] Chiu H C and Yeh C S 2007 *J. Phys. Chem. C* **111** 7256
- [22] Shukla S, Zhang P, Cho H J, Ludwig L and Seal S 2008 *Int. J. Hydrog. Energy* **33** 470
- [23] Suehiro J, Zhou G and Hara M 2003 *J. Phys. D: Appl. Phys.* **36** L109
- [24] Suehiro J, Zhou G, Imakiire H, Ding W and Hara M 2005 *Sensors Actuators B* **108** 398
- [25] Kumar S, Rajaraman S, Gerhardt R A, Wang Z L and Hesketh P J 2005 *Electrochim. Acta* **51** 943
- [26] Suehiro J, Nakagawa N, Hidaka S, Ueda M, Imasaka K, Higashihata M, Okada T and Hara M 2006 *Nanotechnology* **17** 2567
- [27] Suehiro J, Hidaka S I, Yamane S and Imasaka K 2007 *Sensors Actuators B* **127** 505
- [28] Kumar S, Peng Z, Shin H J, Wang Z L and Hesketh P J 2010 *Anal. Chem.* **82** 2204
- [29] Gardeshzadeh A R and Raissi B 2010 *Mater. Sci. Semicond. Process.* **13** 151
- [30] Maeng S et al 2008 *ETRI J.* **30** 516
- [31] Comini E, Faglia G, Sberveglieri G, Pan Z and Wang Z L 2002 *Appl. Phys. Lett.* **81** 1869
- [32] Law M, Kind H, Messer B, Kim F and Yang P 2002 *Angew. Chem. Int. Edn* **41** 2405
- [33] Moon S E et al 2010 *J. Nanosci. Nanotechnol.* **10** 3189
- [34] Wang B, Zhu L F, Yang Y H, Xu N S and Yang G W 2008 *J. Phys. Chem. C* **112** 6643
- [35] Shukla S, Zhang P, Cho H J, Seal S and Ludwig L 2007 *Sensors Actuators B* **120** 573